Infrared and Raman microspectrometry study of fluor-fluor-hydroxy and hydroxy-apatite powders

G. PENEL*†, G. LEROY†, C. REY§, B. SOMBRET#, J. P. HUVENNE# and E. BRES§
* *Laboratoire d'Anatomie bucco-dentaire, Université de Lille II, UFR de Chirurgie-Dentaire, place de Verdun 59000 LILLE, France*
† *U 279 INSERM 1 rue du Prof. Calmette – 59019 LILLE Cedex, France*
§ *Laboratoire des Matériaux – Physico-Chimie des Solides – Ecole Nationale Supérieure de Chimie URA CNRS N°445 – 38, rue des 36 Ponts – 31400 Toulouse, France*
# *LASIR Bât C5 USTL 59655 Villeneuve d'Ascq Cedex, France*
§ *Laboratoire de Metallurgie Physique, LSPES URA CNRS 234, Université de Sciences et Technologie de Lille – Bât C6 – 59650 Villeneuve d'Ascq, France*

Visible Raman and infrared microspectrometry studies performed on fluorapatite and hydroxyapatite powders have shown similar results. Small modifications of the ν_2 and ν_4 PO_4^{3-} tetrahedra bending modes are observed. A small frequency shift of the ν_1 mode and modifications on the ν_3 mode region accompanied with a simplification of the hydroxyapatite and fluorapatite respective spectra from seven to four bands were observed. A broad and weak band which could be attributed to the Ca–F bond is detected at 311 cm^{-1} on the Raman fluorapatite spectra. The phosphate vibration modes are little disturbed by fluoride substitution. This could indicate that phosphate groups interact strongly between themselves and weakly with substituted atoms (i.e. hydroxyle and fluoride atoms). Whatever crystallographic model is considered, the number of bands observed is always lower than the number of calculated ones, even for hydroxyapatite, whose symmetry is lower than that of fluorapatite.

1. Introduction

Hydroxyapatite (OHAp) and its family members are of great interest in biology because they are the main components of bone and teeth. Natural hydroxyapatite is usually found in a crystallized form. OHAp synthesis is a difficult procedure using both hydrothermal [1–3] or aqueous solution [4]. These synthetic compounds are mainly used for surgical implants or bone filling procedures. The chemical composition of OHAp is $Ca_4(I)Ca_6(II)(PO_4)_6(OH)_2$ where the Ca atoms occupy two series of nonequivalent sites; the Ca(I) atoms are on the fourfold symmetry 4(*f*) position and the Ca(II) atoms are in the sixfold symmetry 6(*h*) position. The OH groups occupy disordered positions above or below the triangles formed by the Ca(II) atoms. The disorder of the OH groups gives rise to a "macroscopic" space group $P6_3/m$ (as determined by X-ray diffractometry), which is lost at the level of the individual columns [5].

Depending on the symmetry, some vibrations are Raman active and infrared inactive, and *vice versa*. Hence infrared (IR) and Raman (R) spectrometry give complementary detailed information about molecular vibrations, about the molecular environment, and about the crystallization state of the sample. Infrared spectrometry is a transmission method, so the sample has to be thin. Using a reflection method the Raman microspectrometry allows a direct and non-destructive analysis, so it is possible to obtain a concentration profile of the sample. The spatial resolution (micrometric) of the Raman technique is 100 times higher than the infrared resolution. For all these reasons, Raman microspectrometry is increasingly becoming recognized as a significant method for biomaterials molecular bonds determination and for measurement of the interaction with their environment.

However, Raman microspectrometry cannot give answers to all questions. It gives poor results with amorphous compounds. The Raman signal is about 10^{-6}–10^{-9} times weaker than the excitation, so the detection of any compound with a concentration lower than 1–5% is impossible. The polarization of the laser beam has a strong influence on the intensity of the Raman bands, so it is impossible to obtain strict quantitative compositions of the sample using this method.

2. Materials and methods

2.1. Raman spectrometry

A DILOR OMARS89 microspectrometer with two laser excitation wavelengths, 514 and 632 nm was

0957–4530 © *1997 Chapman & Hall*

used. The spectra were detected by an intensified diode array detector cooled at $-35\,^{\circ}C$. The spectrometer pass band was $2\,cm^{-1}$. Spectra were obtained in the 200–3700 cm^{-1} wave number range. Some spectra were obtained with a DILOR-LABRAM spectrometer.

2.2. Infrared spectrometry

An IRTF Brucker IFS 88 spectrometer with a Brucker A590 microscope was used. With this transmission technique the samples have to be crushed in a mortar and the spectra have to be analysed with a deconvolution method to separate the bands.

2.3. Apatite samples preparation

The following apatite powders were synthesized by methods previously published [6, 7]:

- stoichiometric hydroxyapatite powders (OHAp).
- hydroxyfluorapatite powders (FOHAp).
- fluorapatite powders (FAp).

Stoichiometric hydroxyapatite ($Ca_{10}(PO_4)_6(OH)_2$) powders were prepared by a double decomposition of a calcium nitrate solution (A solution: $Ca(NO_3)_2$, $4H_2O$, prepared using 750 g of $Ca(NO_3)_2$ and 3.3 l of deionized water) and an ammonium phosphate solution (B solution: prepared using 225 g of $(NH_4)_2HPO_4$ and 1.3 l of deionized water). 300 ml of concentrated ammonia was added to the boiling A solution, then solution B was added dropwise to solution A. The mixture was kept boiling for 30 min (maturation procedure). The precipitate was separated by Buchner filtration and washed with deionized water to which was added 5 ml of concentrated ammonia per litre. The precipitate was dried in steam at $70\,^{\circ}C$ for 15 h and heated at $900\,^{\circ}C$ for 2 h. The stoichiometry of the heated sample was checked using X-ray diffraction and infrared spectroscopy.

A similar procedure was used for the fluorapatite $Ca_{10}(PO_4)_6F_2$ and the fluor-hydroxyapatite powders. The same A solution was used. Solution B comprised 225 g of a diammonic ammonium phosphate and 23.5 g and 11.75 g, respectively, of ammonium fluoride in 0.75 l of deionized water to which was added 600 ml of concentrated ammonia. After 1 h precipitation, 100 ml of ammonia was added to the A solution. The precipitates were treated and checked as described above.

3. Results and discussion

3.1. The 400–260 cm^{-1} region (Fig. 1)

The Raman spectral analysis shows a band at 311 cm^{-1} on the fluoride-substituted apatites; this band is observed at 322 cm^{-1} on CaF_2 and was previously reported on FAp at 325 cm^{-1} by Fowler [1] using infrared spectroscopy. This attribution may indicate that the Ca(II)–F bond is partially covalent, like the Ca(II)–OH bond. This observation is consistent with Fowler's OHAp data (the bands at 343 cm^{-1} and

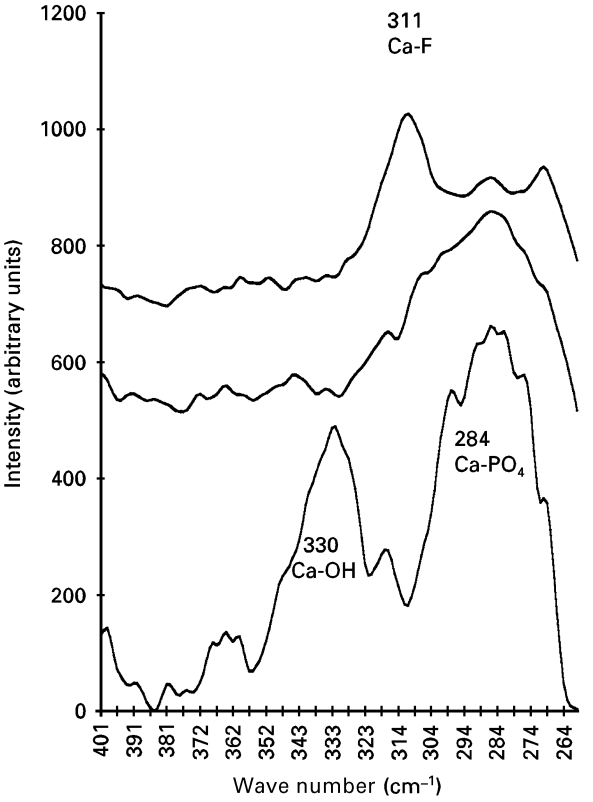

Figure 1 Raman spectra at the low wave number band of the apatitic compounds: stoichiometric hydroxyapatite (OHAp), fluor-hydroxyapatite half substituted (FOHAp), fluorapatite (FAp).

290 cm^{-1} are attributed, respectively, to the Ca(II)–OH and Ca–PO_4 bonds). On the FAp Raman spectra the 333 cm^{-1} frequency band disappears and the 287 cm^{-1} band is weak: they can be attributed to Ca(II)–OH and Ca–PO_4 bonds, respectively. A covalent type bond between the Ca and the F gives higher chemical stability, but the low intensity of this band prevents strict concentration measurement of fluoride in fluoride-substituted apatites.

3.2. The 650–400 cm^{-1} region (Fig. 2)

The ν_2 vibration mode remains constant for the whole substitution range of hydroxyl by fluoride ions; the frequency shift of the bands is identical to the resolution and is hence insignificant. The intensity ratios of the 432 cm^{-1} and 449 cm^{-1} bands are also stable for all apatite powders.

The ν_4 vibration mode exhibits stronger variations. With the second derivative treatment, four bands are seen at the following wave numbers: 581, 592, 608 and 617 cm^{-1}. The first and last decrease as the fluoride content increases, in such a way that the FAp spectra finally show two major bands at 608 and 591 cm^{-1}. The frequency shift between OHAP–FOHAP and FAp is insignificant, considering the slit width of $2\,cm^{-1}$. We have found only two references [3, 8] in which the 617 cm^{-1} band is reported. The 630 or 655 cm^{-1} bands (hydroxyl liberation mode) reported by a number of authors [1, 2, 9, 10] in infrared and Raman spectroscopy, respectively, was not seen in our OHAP, FOHAP and FAp samples. Using

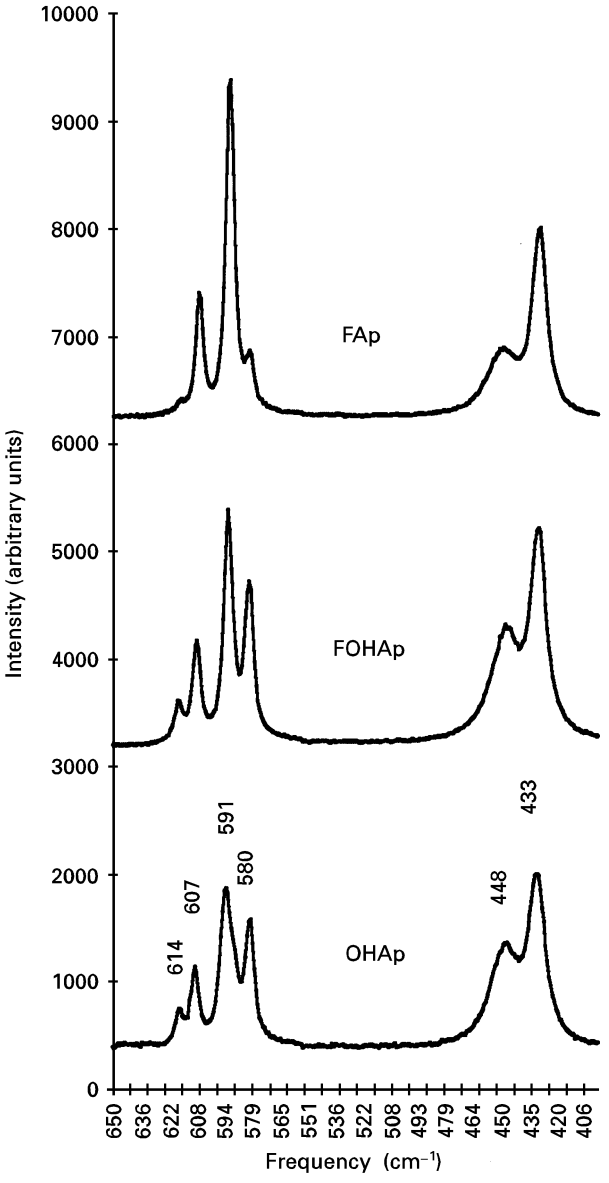

Figure 2 Raman spectra of the ν_2 and ν_4 phosphate mode region of the apatitic compounds.

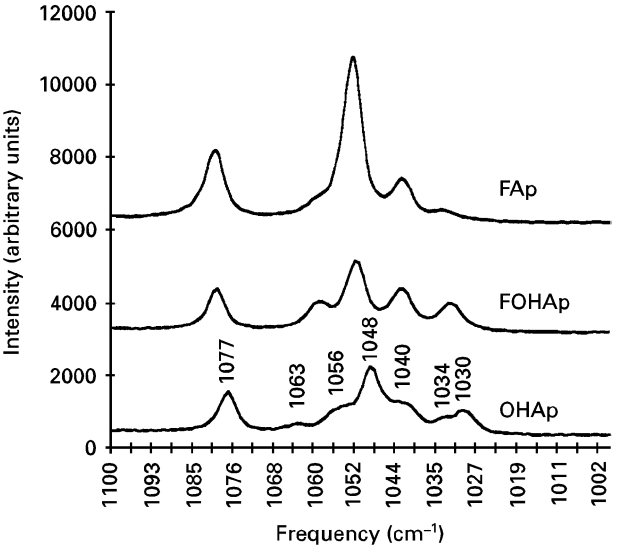

Figure 3 Raman spectra of the ν_3 mode region of the phosphate.

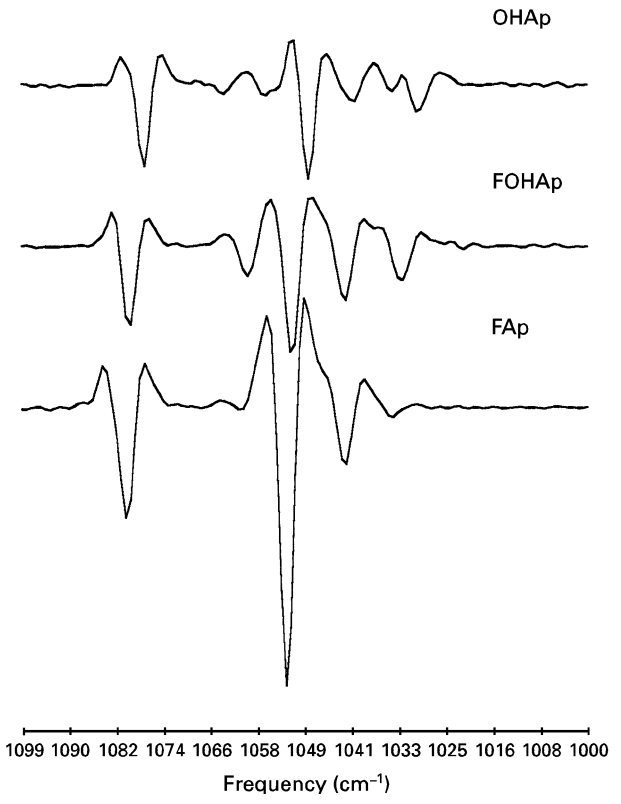

Figure 4 Second derivative function of the ν_3 mode region of the phosphate.

infrared spectroscopy Freund [10] described a correlation between the gradual introduction of fluoride in OHAp and the increase of intensity of a band around 720–740 cm^{-1} and the decrease of intensity of the 630 cm^{-1} band.

3.3. The 1100–900 cm^{-1} region

In the ν_1 phosphate mode region, the slight frequency shift from 963 cm^{-1} to 965 cm^{-1}, equal to the slit width, is insignificant. The three samples show bands of the same intensity.

As opposed to the other phosphate modes, ν_3 exhibits strong variations upon fluoride substitutions (Fig. 3). In the second derivative of the OHAp spectra (Fig. 4) seven bands previously reported by Nelson [8] are clearly distinguished at the following wave numbers: 1030, 1034, 1040, 1048, 1056, 1063 and 1077 cm^{-1}. Five bands are observed in the FOHAp at the following wave numbers: 1032, 1042, 1051, 1059 and 1080 cm^{-1}.

Only four bands were found in FAp, at the following wave numbers: 1034 (very weak), 1042, 1053 and 1081 cm^{-1}. A significant frequency shift, close to 5 cm^{-1}, appears with fluoride substitution.

If we consider these results and X-ray and neutron diffraction data, we can form the hypothesis that FAp has less lattice strain than OHAp. This is consistent with the fact the fluoride atom is smaller than the OH group, and has a symmetrical configuration inside the Ca(II) triangle along the *c* axis. OHAp and FAp have hexagonal structures with respective space groups: $P6_3$ and $P6_3/m$. Neutron diffraction data showed that the OH groups are displaced about

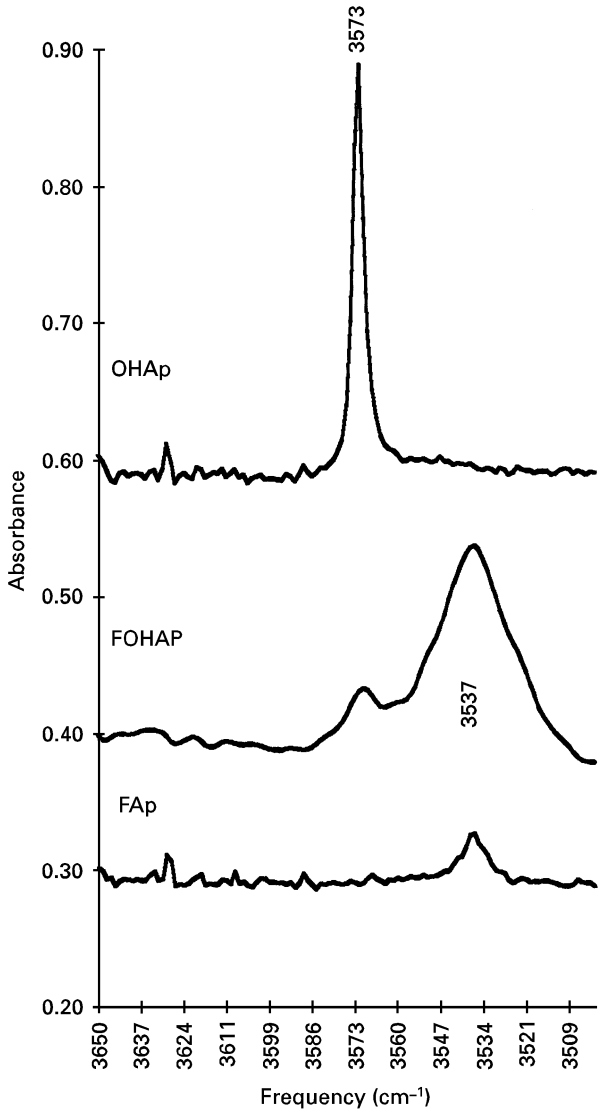

Figure 5 Infrared spectra of the OH stretching mode region of the apatitic compounds.

0.03 nm above or below the mirror plane at $z = 1/4$ and $z = 3/4$ where the triangles formed by the Ca_{II} atoms are located [5].

3.4. The 3510–3650 cm^{-1} region (Fig. 5)

In this region the PO_4^{3-} vibrations have no influence on the OH mode since they are separated by the ionic bonds of the calcium II. Consistent with the literature, we observe a single band in OHAp at 3573 cm^{-1}. In FOHAp we observe two bands at the following wave numbers: 3573 and 3537 cm^{-1}. Attribution of these bands has been discussed by Freund *et al.* [10]. The infrared spectra of the FAp sample shows a weak band at 3537 cm^{-1}, likely due to an incomplete substitution of OH during the synthesis procedure. This band is also reported on natural FAp [1].

3.5. Discussion

We now focus attention on the phosphate vibration modes. All spectra are normalized such that the ν_1 intensity remains constant. It has to be noted that as the number of bands decreases (ν_3 and ν_4), the intensity and the remaining bands increases; higher crystallographic symmetry could explain this result (see Table I).

TABLE I Phosphate and hydroxyl vibration modes in the apatitic samples

Vibration mode	Vibration frequency (cm^{-1}) Fluorapatite (FAp)	Hydroxyfluorapatite (FOHAp)	Hydroxyapatite (OHAp)
PO_4 ν_1	965	963	963
PO_4 ν_2	432	431	433
	449	446	448
PO_4 ν_3			1029
	1034	1032	1034
	1042	1042	1041
	1053	1051	1048
	1061	1059	1057
			1064
	1081	1080	1077
PO_4 ν_4	581	580	580
	592	590	591
	608	606	607
	615	615	614
OH ν_1	3540	3540	
		3560	
		3570	3573

The number of bands predicted for the $P6_3/m$ (C_{6h}) space group by group theoretical methods is five for ν_3 and ν_4 modes, three for ν_2 and two for ν_1 [1, 11]. As the space group is centro-symmetric, the IR bands are active when the Raman bands are inactive, and vice versa. For the $P6_3$ space group (C_6 group factor) the predicted number of Raman active bands is nine for ν_3 and ν_4 modes, six for ν_2 mode and three for ν_1 mode [3] (Table II). FOHAp should not have a $P6_3$ space group (C_6 group factor) because of the two types of ionic substitution; only the C_3 symmetry axis should be preserved. Under these conditions, coupling of the phosphate groups in the planes at 1/4 and 3/4 should be lost and we should observe on the Raman spectra twelve bands for ν_3 and ν_4 modes (six for each 1/4 and 3/4 group), eight bands for ν_2 mode (four for each group) and four bands for ν_1 mode (two for each group). This is not shown in our experimental data, particularly on the phosphate mode region of FAp and OHAp spectra where our data are similar. On the other hand, our data seem to be consistent with a higher symmetry and confirm the space group used for the spectral attribution, even if not all the predicted bands are observed in our samples. The similarity between FAp and FOHAp spectra shows that the increase of symmetry has only a small influence on the phosphate vibration modes, even if the FOHAp spectra seem to be simpler than the OHAp spectra.

Hence monovalent ionic substitutions seem to have only a small influence on phosphate group coupling in apatites in which the mirror plane is lost. In other words, in these compounds, if we assume:

- strong coupling between the three phosphate groups of the 1/4 and 3/4 planes, which present a symmetry close to $\overline{6}(C_{3h})$;

TABLE II Raman and IR vibration modes of PO_4^{3-} (OS: out of scale, NO: not observed)

			Wave number (cm^{-1})				
	C_{3h}	C_{6h}	Klee Raman [10]	Present work Raman	Klee IR [10]	Present work IR	Comment
ν_1	A′E′	A_gE_{2g} E_{1u}	963	965	962	965	Close to C_{3h}
ν_2	E″	E_{1g}	429	432			Close to C_{6h}
		E_{2g}	446				
	A′	A_g	451	449			
	E′ or A″	E_{1u}	NO	NO	460	OS	
	A″ or E′	A_u			470	473	
ν_3	E″	A_uE_{2g}	1033	1034	(1032)		Between C_{6h} and C_{3h}
	E′	$E_{1g}E_{1u}$	1040	1042	1040	1044	
	A′	A_g	1051	1053			
	E′	E_{2g}	1059	1061		NO	
	A′	A_g	1078	1081			
	A″	E_{1u}			1090	1095	
ν_4		A_u			(560)		( ) CO_3
	A″	E_{1u}			575	575	Close to C_{6h}
	E′	E_{2g}	580	581		NO	
	A′	A_gE_{1g}	591	592			
	E′	E_{1u}	NO	NO	601	603	
	A′	A_g	606	608			
	E″	E_{2g}	615	617			

TABLE III Correlation table for the phosphate ions with different local symmetry (R: Raman active, IR: infrared active)

Local group symmetry	Vibration modes of free ion (T_d group)	Site symmetry (C_1 or C_S)	Vibration modes of the ion in the crystal	Comments
C_{6h}	$A_1(\nu_1)$	A′	A_g(R); E_{2g}(R); B_u; E_{1u}(IR)	This local group is the group factor of the $P6_{3/m}$ space group
	$E(\nu_2)$	A′	A_g(R); E_{2g}(R); B_u; E_{1u}(IR)	
		A″	B_g; E_{1g}(R); A_u(IR); E_{2u}	
	$T_2(\nu_3$ or $\nu_4)$	2A′	$2A_g$(R); $2E_{2g}$(R); $2B_u$; $2E_{1u}$(IR)	
		A″	B_g; E_{1g}(R); A_u(IR); E_{2u}	
C_6	$A_1(\nu_1)$	A	A(IR, R); E_1(IR, R); B; E_2(R)	This local group is the group factor of the $P6_3$ space group
	$E(\nu_2)$	2A	2A(IR, R); $2E_1$(IR, R); 2B; $2E_2$(R)	
	$T_2(\nu_3$ or $\nu_4)$	3A	3A(IR, R); $3E_1$(IR, R); 3B; $3E_2$(R)	
C_3	$A_1(\nu_1)$	A	A(IR, R); E(IR, R)	This symmetry corresponds with loss of the phosphate groups in plane at 1/4 and 3/4 coupling and with a C_1 symmetry
	$E(\nu_2)$	2A	2A(IR, R); 2E(IR, R)	
	$T_2(\nu_3$ or $\nu_4)$	3A	3A(IR, R); 3E(IR, R)	
C_{3h}	$A_1(\nu_1)$	A′	A′(R); E′(IR, R)	This symmetry corresponds with loss of the phosphate groups in plane at 1/4 and 3/4 coupling with a C_s symmetry.
	$E(\nu_2)$	A′	A′(R); E′(IR, R)	
		A″	A″(IR); E″(R)	
	$T_2(\nu_3$ or $\nu_4)$	2A′	2A′(R); 2E′(IR, R)	
		A″	A″(IR); E″(R)	

- these two groups of phosphates have a very similar environment leading to similar wave number vibration modes,

we can compare the predicted spectra and the observed spectra in five bands for the ν_3 and the ν_4 modes, three bands for the ν_2 mode and two bands for the ν_1 mode. This hypothesis also can predict the IR spectra: three bands for the ν_3 and ν_4 modes, including two bands, with identical wave number in IR and Raman spectra; two bands for the ν_2 mode, including one IR and Raman common band; and one band for the ν_1 mode. This hypothesis is very helpful in describing the strong bands observed in the apatite spectra. It seems that the consistent symmetry change of the FAp from $\bar{6}(C_{3h})$ to $6/m(C_{6h})$ (Table III). This hypothesis is not in agreement with data published on natural FAp single crystals (which is not pure FAp) so we need further experimentation to support such a hypothesis.

Comparison with Klee [12] and Kravizt [13] data highlights problems that local symmetry

considerations cannot solve (Table III). For example, for the ν_3 mode, if a C_{6h} point group is accepted, different bands should not have common IR and Raman wave numbers: A_u and E_{2g} at 1033 cm^{-1}, E_{1g} and E_{1u} at 1042 cm^{-1}. Moreover, the 1033 cm^{-1} band is always observed in the IR spectra. The same problem is encountered with the ν_4 A_u band at 560 cm^{-1}. Might they be specific to natural carbonated FAp? On the other hand, the predicted ν_2 bands of the C_{6h} point group are consistent with the IR and Raman spectra observed. For the ν_1 mode, the three bands (A_g, E_{2g} and E_{1u}) are all observed at the same wave number in both IR and Raman spectra. Hence some unsolved problems persist with the $6/m(C_{6h})$ space group.

If we consider the $\bar{6}(C_{3h})$ point group, with the phosphate positions at z = 1/4 and 3/4, then, consistent with the published data and the bands observed, the ν_1 region exhibits two vibration modes: A′ and E′. In contrast, for the ν_2 mode region, the E_{2g} (446 cm^{-1}) and the A_g (451 cm^{-1}) bands should be considered as a A′ single band, and a Raman active band should appear around 470 cm^{-1} (E′). In the ν_3 mode region, the IR E_{1u} band (1090 cm^{-1}) should become an A″ mode because it has never been observed in the Raman spectra, and we have to consider that the IR 1032 cm^{-1} band should not exist. However, an IR band should be observed at 1060 cm^{-1}. For the ν_4 mode the IR band at 560 cm^{-1} also should not exist, and the 575 cm^{-1} band should be an A″ mode. In this case, the IR active band at 601 cm^{-1} should be common with a Raman band: this has never been observed (see Table II).

For OHAp, very few modifications are observed in the ν_1, ν_2 and ν_4 modes. In contrast, the ν_3 mode exhibits seven bands in our samples (powder). These seven bands are observed in samples using two different synthesis procedures and in Bioapatite (PRED®). The results are not perfectly consistent with observations on single crystals, where only six bands are observed [14]. Even if there is no doubt about these data, small modifications appear in the band attribution of FAp to OHAp: for ν_2 the E_{1g} (427 cm^{-1}) in FAp becomes E_1, A (432 cm^{-1}) in OHAp; for the ν_4 mode, the A_g (605 cm^{-1}) in FAp becomes A, E_2 (609 cm^{-1}) in OHAp; and for the ν_3 mode the A_g (1082 cm^{-1}) in FAp becomes A, E_2 (1077 cm^{-1}) in OHAp.

Finally, Raman microspectrometry has to be considered as a very interesting technique, which gives new and complementary results about composition and crystallization of apatitic compounds. However, complete attribution of bands is not possible because of the difficulties encountered in producing absolutely pure samples.

Acknowledgements

The authors wish to thank Paolo Valisa and the DILOR Corporation for their collaboration and support.

References

1. B. O. FOWLER, *Inorg. Chem.* **13** (1974) 194–207.
2. K. C. BLAKESLEE and R. A. CONDRATE, SR. *J. Amer. Ceram. Soc.* **54** (1971) 559–563.
3. D. C. O'SHEA, M. L. BARETLETT and R. A. YOUNG, *Arch. Oral Biol.* **19** (1974) 995–1006.
4. J. ARENDS, J. CHRISTOFFERSEN, M. R. CHRISTOFFERSEN, H. ECKERT, B. O. FOWLER, J. C. HEUGHEBAERT, G. H. NANCOLLAS, J. P. YESINOWSKI and S. J. ZAWACKI, *J. Cryst. Growth* **84** (1987) 515–532.
5. M. I. KAY, R. A. YOUNG and A. S. POSNER, *Nature* **204** (1964) 1050–1052.
6. C. REY, M. SHIMIZU, B. COLLINS and M. J. GLIMCHER, *Calcif. Tissue Int.* **49** (1991) 383–388.
7. *Idem., ibid.* **46** (1990) 384–394.
8. D. G. A. NELSON and B. E. WILLIAMSON, *Aust. J. Chem.* **35** (1982) 715–727.
9. B. O. FOWLER, E. C. MORENO and W. E. BROWN, *Arch. Oral Biol.* **11** (1966) 477–492.
10. F. FREUND and R. M. KNOBEL, *J. Chem. Soc.* **6** (1977) 1136–1140.
11. J. C. TROMBE and G. MONTEL, *C.R. Acad. Sci. Paris* **276** (1973) 1271–1274.
12. W. E. KLEE *Zeitschrif für Kristallographie* **131** (1970) 95–102.
13. L. C. KRAVITZ, J. D. KINGSLEY and E. L. ELKIN, *J. Chem. Phys.* **49** (1968) 4600–4610.
14. H. TSUDA and J. ARENDS, *J. Dent. Res.* **11** (1994) 1703–1710.

Received 19 April
and accepted 29 May 1996